

**Project Report  
ATC-336**

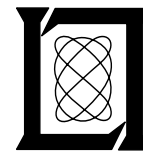
# **Evaluation of Potential NEXRAD Dual Polarization Products**

D.J. Smalley

4 September 2007

---

**Lincoln Laboratory**  
MASSACHUSETTS INSTITUTE OF TECHNOLOGY  
*LEXINGTON, MASSACHUSETTS*



---

Prepared for the Federal Aviation Administration,  
Washington, D.C. 20591

This document is available to the public through  
the National Technical Information Service,  
Springfield, Virginia 22161

This document is disseminated under the sponsorship of the Department of Transportation, Federal Aviation Administration, in the interest of information exchange. The United States Government assumes no liability for its contents or use thereof.

1. Report No. ATC-336	2. Government Accession <sup>3</sup> No.	3. Recipient's Catalog No.	
4. Title and Subtitle Evaluation of Potential NEXRAD Dual Polarization Products		5. Report Date 4 September 2007	
		6. Performing Organization Code	
7. Author(s) David J. Smalley		8. Performing Organization Report No. ATC-336	
9. Performing Organization Name and Address MIT Lincoln Laboratory 244 Wood Street Lexington, MA 02420-9108		10. Work Unit No. (TRAIS)	
		11. Contract or Grant No. FA8721-05-C-0002	
12. Sponsoring Agency Name and Address Department of Transportation Federal Aviation Administration 800 Independence Ave., S.W. Washington, DC 20591		13. Type of Report and Period Covered Project Report	
		14. Sponsoring Agency Code	
15. Supplementary Notes  This report is based on studies performed at Lincoln Laboratory, a center for research operated by Massachusetts Institute of Technology, under Air Force Contract FA8721-05-C-0002.			
16. Abstract  The NEXRAD program will begin fielding a dual polarization capability in 2009. Three additional base data parameters and two additional derived parameters from the dual polarization capability will be produced to complement the traditional three radar moments. The initial use of the added data is to provide a dual-polarization-based quantitative precipitation estimate (QPE) algorithm. Other NEXRAD algorithms will have access to the new dual polarization parameters as well as the derived products.  The National Severe Storms Laboratory coordinated a dual polarization product evaluation to solicit NEXRAD agency participant feedback regarding potential dual polarization products. The evaluation consisted of analyzing dual polarization data from seven weather cases. MIT Lincoln Laboratory participated in the evaluation. The evaluation opportunity was used to have early access to prototypical dual polarization data to consider the potential benefit to FAA weather systems. This report introduces the new dual polarization parameters, presents some of the relevant weather cases, and provides recommendations regarding use of the dual polarization parameters.			
17. Key Words		18. Distribution Statement  This document is available to the public through the National Technical Information Service, Springfield, VA 22161.	
19. Security Classif. (of this report) Unclassified	20. Security Classif. (of this page) Unclassified	21. No. of Pages 32	22. Price

## EXECUTIVE SUMMARY

The NEXRAD program will begin fielding a dual polarization capability in 2009. Three additional base data parameters from the dual polarization capability will be produced to complement the traditional three radar moments. At least two additional derived parameters will also be produced. The initial use of the added data is to provide a dual-polarization based quantitative precipitation estimate (QPE) algorithm. This algorithm was developed by the National Severe Storms Laboratory (NSSL). The process of transitioning this algorithm to NEXRAD has ensured that other NEXRAD algorithms will have access to the new dual polarization parameters as well as the derived products.

The NSSL coordinated a dual polarization product evaluation for NEXRAD tri-agency participants. The purpose of the evaluation was to solicit participant feedback regarding potential dual polarization products for NEXRAD through analysis of dual polarization data from seven weather cases. The feedback is being used to define the initial set of new dual polarization products for NEXRAD. Participants were requested to focus on the display of the products rather than the correctness of any underlying algorithm. Evaluation results suggest that many in the operational meteorological community will need to build a familiarity and understanding of the new dual polarization products' capabilities. Building confidence in these capabilities will also be necessary.

MIT Lincoln Laboratory participated in the NSSL-coordinated evaluation. Feedback of the type requested was provided. The opportunity was also used to have early access to prototypical dual polarization data to consider the potential benefit to FAA weather systems. The key observations are:

- ✓ Many more weather cases with dual polarization data are needed from many regions of the United States
- ✓ Data quality techniques may benefit from incorporation of hydrometeor classification information
- ✓ The connection between surface conditions (such as for terminal operations) and hydrometeor classification is uncertain
- ✓ The new dual polarization parameters will benefit FAA weather systems only after new, automated algorithms are fielded



## TABLE OF CONTENTS

	<b>Page</b>
EXECUTIVE SUMMARY	iii
List of Illustrations	vii
1. INTRODUCTION	1
2. DUAL POLARIZATION AND DERIVED DUAL POLARIZATION PARAMETERS	3
2.1 Differential Reflectivity ( $Z_{DR}$ )	3
2.2 Differential Phase Shift ( $\phi_{DP}$ )	3
2.3 Correlation coefficient ( $\rho_{HV}$ )	3
2.4 Hydrometeor Classification	3
2.5 Specific differential phase shift ( $K_{DP}$ )	4
3. SAMPLE CASES	5
3.1 Squall Line	5
3.2 Snowfall	8
3.3 Light Rain and Bright Band	11
3.4 Freezing Rain	15
4. SUMMARY	19
GLOSSARY	21
REFERENCES	23



## LIST OF ILLUSTRATIONS

Figure No.		Page
1a	Traditional reflectivity (dBZ) from the base tilt of the radar volume collected on June 11, 2003 at 0254 UTC.	5
1b	Differential reflectivity (dB) from the base tilt of the radar volume collected on June 11, 2003 at 0254 UTC.	6
1c	Hydrometeor classification results for the base tilt of the radar volume collected on June 11, 2003 at 0254 UTC.	6
1d	Specific differential phase shift ( $K_{DP}$ ) in units of degrees/km for the base tilt of the radar volume collected on June 11, 2003 at 0254 UTC.	7
1e	Correlation coefficient ( $\rho_{HV}$ ) for the base tilt of the radar volume collected on June 11, 2003 at 0254 UTC.	7
2a	Traditional reflectivity (dBZ) from the base tilt of the radar volume collected on December 22, 2004 at 1556 UTC.	9
2b	Differential reflectivity (dB) from the base tilt of the radar volume collected on December 22, 2004 at 1556 UTC.	9
2c	Hydrometeor classification results for the base tilt of the radar volume collected on December 22, 2004 at 1556 UTC.	10
2d	Specific differential phase shift ( $K_{DP}$ ) in units of degrees/km for the base tilt of the radar volume collected on December 22, 2004 at 1556 UTC.	10
2e	Correlation coefficient ( $\rho_{HV}$ ) for the base tilt of the radar volume collected on December 22, 2004 at 1556 UTC.	11
3a	Traditional reflectivity (dBZ) from the 1.45° tilt of the radar volume collected on May 2, 2005 at 1618 UTC.	12
3b	Differential reflectivity (dB) from the 1.45° tilt of the radar volume collected on May 2, 2005 at 1618 UTC.	13



**LIST OF ILLUSTRATIONS**  
**(Continued)**

<b>Figure No.</b>		<b>Page</b>
3c	Hydrometeor classification results for the 1.45° tilt of the radar volume collected on May 2, 2005 at 1618 UTC.	13
3d	Specific differential phase shift ( $K_{DP}$ ) in units of degrees/km for the 1.45° tilt of the radar volume collected on May 2, 2005 at 1618 UTC.	14
3e	Correlation coefficient ( $\rho_{HV}$ ) for the 1.45° tilt of the radar volume collected on May 2, 2005 at 1618 UTC.	14
4a	Traditional reflectivity (dBZ) from the base tilt of the radar volume collected on January 5, 2005 at 0541 UTC.	15
4b	Differential reflectivity (dB) from the base tilt of the radar volume collected on January 5, 2005 at 0541 UTC.	16
4c	Hydrometeor classification results for the base tilt of the radar volume collected on January 5, 2005 at 0541 UTC.	16
4d	Specific differential phase shift ( $K_{DP}$ ) in units of degrees/km for the base tilt of the radar volume collected on January 5, 2005 at 0541 UTC.	17
4e	Correlation coefficient ( $\rho_{HV}$ ) for the base tilt of the radar volume collected on January 5, 2005 at 0541 UTC.	17

## 1. INTRODUCTION

The NEXRAD program will begin fielding a dual polarization capability in 2009. In addition to the traditional three radar moments now collected, three dual polarization parameters will also be collected. They are differential reflectivity ( $Z_{DR}$ ), differential phase shift ( $\Phi_{DP}$ ), and correlation coefficient ( $\rho_{HV}$ ). The initial release of the dual polarization capability in NEXRAD will include a dual-polarization based quantitative precipitation estimate (QPE) algorithm developed by the National Severe Storms Laboratory (NSSL).

The NSSL dual polarization QPE algorithm was developed outside of the NEXRAD environment using dual polarization data collected by a non-NEXRAD-standard radar. The algorithm uses the dual polarization parameters as well as some additional derived dual polarization parameters. Two notable derived parameters are HCA (hydrometeor classification) and  $K_{DP}$  (the specific differential phase shift). The NEXRAD Dual Polarization Software Design Working Group was formed to guide the integration of the algorithm into the NEXRAD program. The design process has ensured that other NEXRAD algorithms will have access to the new dual polarization parameters as well as derived products that are initially associated with the NSSL QPE algorithm. This access will not be with the first release, however.

The integration effort led to the determination of which dual polarization products and data would be available in the NEXRAD Open Radar Product Generator (ORPG). The NSSL coordinated a dual polarization product evaluation for NEXRAD tri-agency participants to have a first look at the new dual polarization data and derived products. Participants were requested to focus on the display of the products rather than the correctness of any underlying algorithm. Seven dual polarization weather cases were provided for analysis via the WDSS-II, Warning Decision Support System - Integrated Information (Lakshmanan, *et al.*, 2007). The data provided included reflectivity, the dual polarization parameters, derived dual polarization parameters, and precipitation accumulation parameters. Doppler data were not available. The weather cases generally were of events with durations as much as a few hours. Weather phenomena represented include supercell thunderstorms, squall lines, snow, light rain, and mixed-phase precipitation at various ranges from the radar. Supporting synoptic and mesoscale surface observations provided aid for the interpretation of the radar data. A complete description of the evaluation is provided by Scharfenberg and Manross (2007).

MIT Lincoln Laboratory participated in the evaluation specifically to begin assessing the potential benefit to FAA weather systems of NEXRAD dual polarization data. This document includes brief introductions of the dual polarization parameters and derived dual polarization parameters that will be available in NEXRAD. Samples from the evaluation case set are presented. A summary discussion completes the document.



## 2. DUAL POLARIZATION AND DERIVED DUAL POLARIZATION PARAMETERS

With dual polarization, the new information acquired relates to the size distribution and characteristics of scatterers in a given sample volume as remotely sensed by pulses of differing, orthogonal polarity. NEXRAD will transmit simultaneous linear horizontal and vertical pulses. The lesser precipitation scatterers are spherical (increasingly larger drops), the greater the differences in returned power and phase from the different polarity pulses. The principle dual polarization parameters are estimates of those differing returns. The derived dual polarization parameters effectively gather the dual polarization data into a combined form more conducive for some applications. Bringi and Chandrasekar (2001) and many others provide in-depth discussion of these parameters. While beyond the scope of this document, it should be noted that radar calibration takes on added importance when considering using dual polarization parameters. The following are summary introductions to the parameters.

### 2.1 DIFFERENTIAL REFLECTIVITY ( $Z_{DR}$ )

$Z_{DR}$  is ten times the log of the ratio of the horizontal and vertical reflectivity return from a sample volume. Large drops are oblate spheroids and have increasingly larger returns from the horizontal pulses compared with the vertical pulses. For  $Z_{DR}$  over 6 dB, the drop diameters are exceeding 8 mm. Drops with diameters under about 0.5 mm have  $Z_{DR}$  about zero. Unfortunately, hail has a  $Z_{DR}$  of around zero also. Generally, snow has a low  $Z_{DR}$  independent of shape due to its small dielectric constant (Salek, 2004).

### 2.2 DIFFERENTIAL PHASE SHIFT ( $\Phi_{DP}$ )

$\Phi_{DP}$  is the difference in the returned phase of the vertical and horizontal returns. The difference in return phase is greater from areas of large oblate spheroid drops because the horizontal pulses are slowed slightly more than the vertical pulses. This slight difference is enhanced by range from the radar. It is generally regarded that  $\Phi_{DP}$  is best used in its range derivative form  $K_{DP}$ .

### 2.3 CORRELATION COEFFICIENT ( $\rho_{HV}$ )

$\rho_{HV}$  is a measure of the correlation of the returned power from the horizontal and vertical pulses. Typical meteorological values are near unity with a very small dynamic range. In regions of non-uniform scatterers, such as mixed phase areas (i.e. – melting layers), the  $\rho_{HV}$  is lower. Ground clutter and regions of AP also have lower values.

### 2.4 HYDROMETEOR CLASSIFICATION

The ability to classify the bulk precipitation scatterers of a sample volume through analysis of dual polarization parameters is a key capability added from the NEXRAD dual polarization upgrade. The new

information can be used for purposes of improving data quality to enhanced QPE. The latter will be the first use of the capability in NEXRAD. Ryzhkov *et al.* (2005) describe the general concept of the fuzzy logic system used to determine scatterer classes. Scharfenberg and Manross (2007) include more references concerning the functionality of the hydrometeor classification. Research continues in this field. Currently, about twelve classes are expected.

## **2.5 SPECIFIC DIFFERENTIAL PHASE SHIFT ( $K_{DP}$ )**

$K_{DP}$  is the range derivative of  $\Phi_{DP}$ . It is generally immune to large hail and thus is considered a useful indicator of actual rain rates. Larger values indicate higher rain rates. In light rain, non-oblate spheroids result in very little return phase differences.

### 3. SAMPLE CASES

Seven cases from central Oklahoma were provided for evaluation. Figures 1 through 4 show representative samples from four of the cases. Each figure is a set of five panels (a through e). The panels are a) traditional reflectivity, b) differential reflectivity ( $Z_{DR}$ ), c) hydrometeor classification (HCA), d) specific differential phase shift ( $K_{DP}$ ), and e) correlation coefficient ( $\rho_{HV}$ ). The cases, as presented here, allow for limited inspection but are chosen to highlight certain pertinent observations. The WDSS-II GUI application used for the evaluation provides a means to explore the vertical structure and time series evolution of the weather that is not easily captured for this document. For FAA weather systems to benefit from the NEXRAD dual polarization upgrade, new automated algorithms that analyze the vertical structure and time series evolution of the weather remotely-sensed with dual polarization will need to be developed.

#### 3.1 SQUALL LINE

Figure 1 shows a squall line of strong convection from June 11, 2003 at 0254 UTC. All panels are from the base tilt of the radar volume. An outflow boundary in front of the strong convective cells is southeast of the radar. The yellow and red regions along the squall line seen in the  $Z_{DR}$  panel (b) indicate large diameter droplets.  $K_{DP}$  (panel d) shows highest values in cells embedded along the leading edge of the squall line. Those regions likely have the highest rain rates occurring. The correlation coefficient ( $\rho_{HV}$ , panel e) shows near unity values corresponding to the squall line with much lower values centered near the radar associated with clutter and anomalous propagation (AP) post squall line passage.

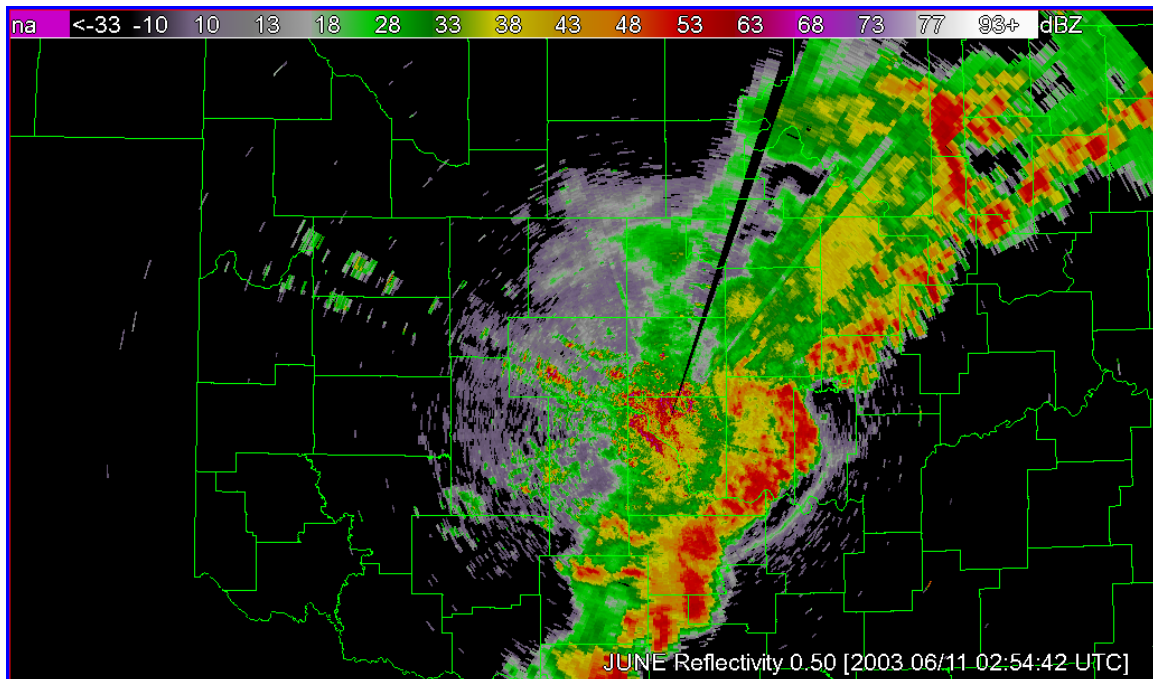


Figure 1a. Traditional reflectivity (dBZ) from the base tilt of the radar volume collected on June 11, 2003 at 0254 UTC. The scene depicts a squall line with a leading outflow boundary. Refer to section 3.1 for more detail.

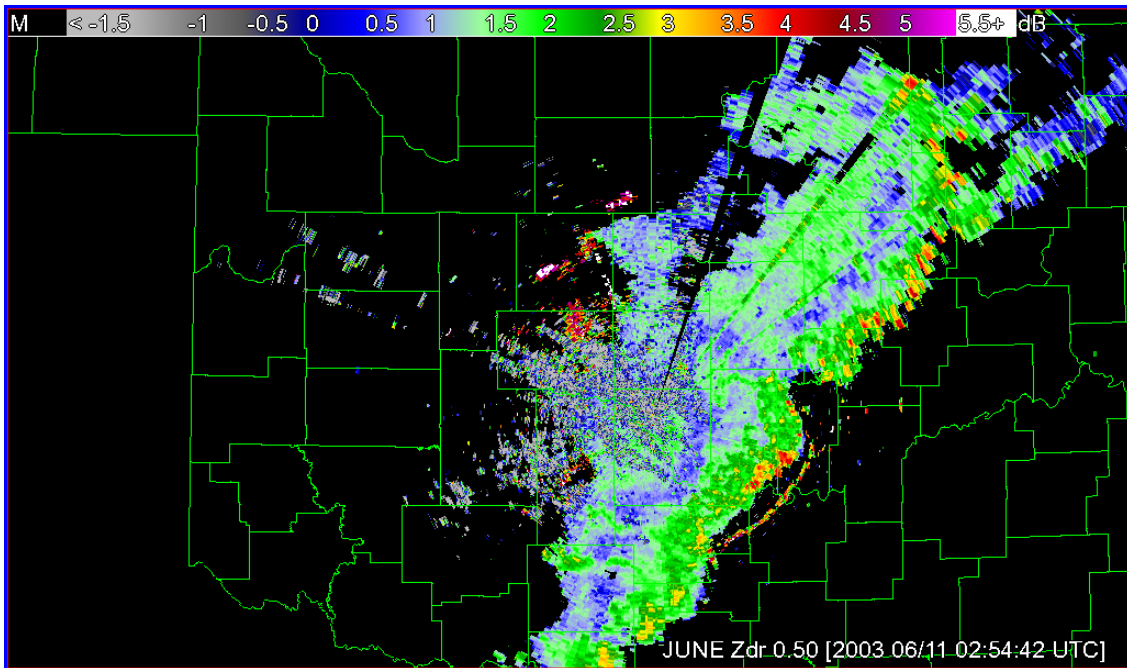


Figure 1b. Differential reflectivity (dB) from the base tilt of the radar volume collected on June 11, 2003 at 0254 UTC. The scene depicts a squall line with a leading outflow boundary. Regions of yellow/red indicate the likely presence of large drops. Refer to section 3.1 for more detail.

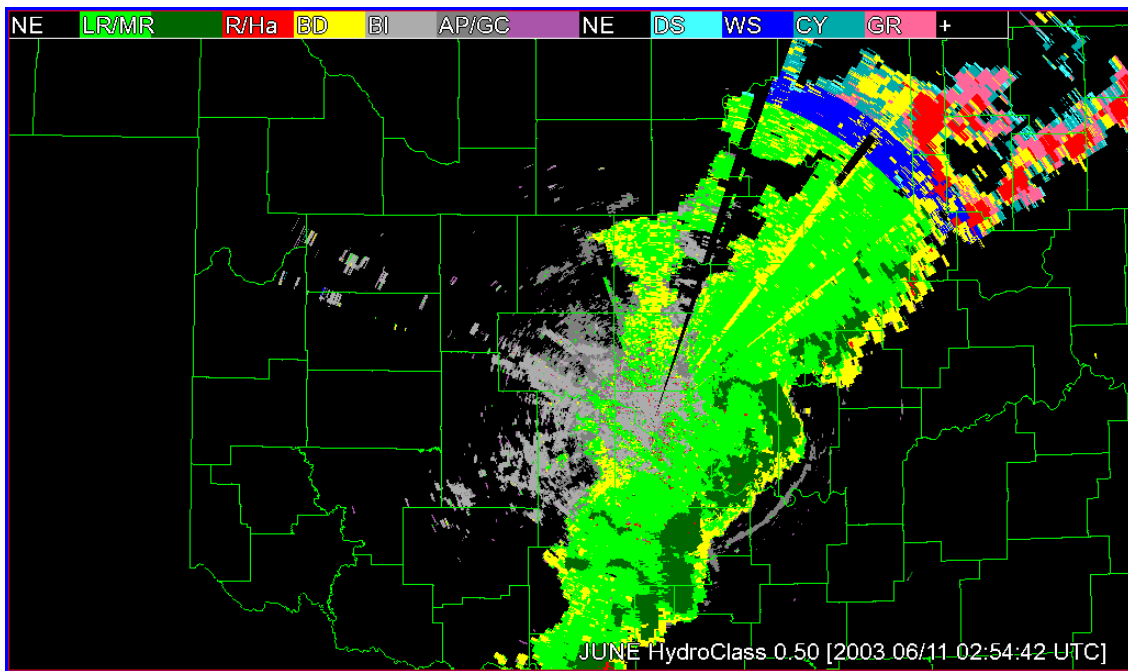


Figure 1c. Hydrometeor classification results for the base tilt of the radar volume collected on June 11, 2003 at 0254 UTC. The scene depicts a squall line with a leading outflow boundary. That outflow is classified as AP. Decode the color scale as follows: black (NE – no echo), light green (LR – light rain), dark green (MR – medium intensity rain), red (R/Ha – heavy rain and/or hail), yellow (BD – big drops), gray (BI – biological targets), dark gray (AP – anomalous propagation), lavender (GC – ground clutter), light blue (DS – dry snow), dark blue (WS – wet snow), cyan (CY – ice crystals), and pink (GR – graupel). Refer to section 3.1 for more detail.

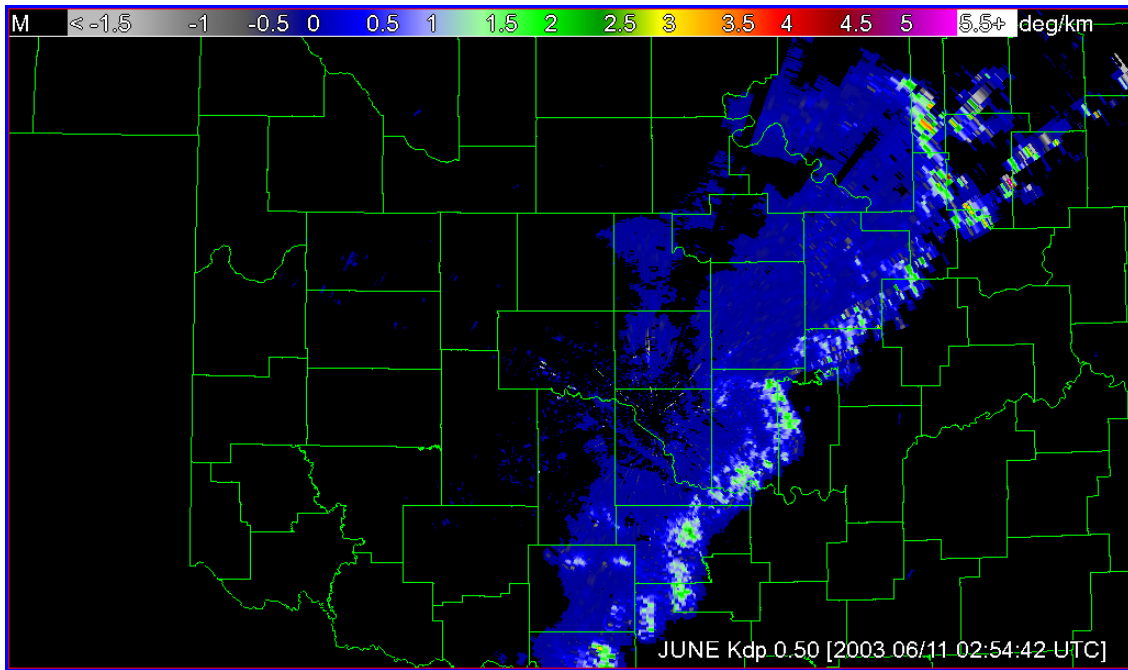


Figure 1d. Specific differential phase shift ( $K_{DP}$ ) in units of degrees/km for the base tilt of the radar volume collected on June 11, 2003 at 0254 UTC. The scene depicts a squall line with a leading outflow boundary. High values are indicative of relatively higher rain rates. Refer to section 3.1 for more detail.

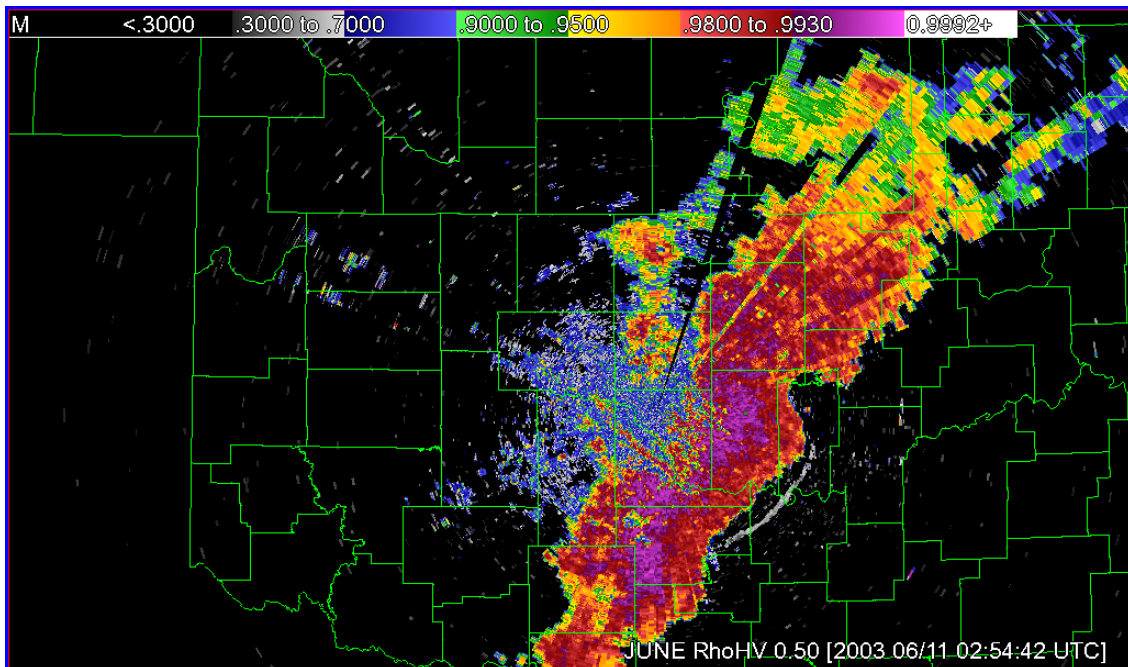


Figure 1e. Correlation coefficient ( $\rho_{HV}$ ) for the base tilt of the radar volume collected on June 11, 2003 at 0254 UTC. The scene depicts a squall line with a leading outflow boundary. This field has a small dynamic range near unity. Refer to section 3.1 for more detail.



The hydrometeor classification parameter (panel c) has the classes color coded as follows:

- light green signifies light intensity rain (LR),
- darker green signifies medium intensity rain (MR),
- red signifies strong intensity rain and/or hail (R/Ha),
- yellow represents big drops (BD),
- gray represents biological scatterers (BI),
- darker gray represents AP (AP),
- lavender indicates ground clutter (GC),
- light blue indicates dry snow (DS),
- dark blue indicates wet snow (WS),
- cyan signifies crystals (CY), and
- pink represents graupel (GR).

In this case, the squall line is classified by the varying rain intensities. Near the radar AP and biological targets are found. Interestingly, the outflow boundary is classified as AP. The use of the BI, AP, and GC categories is expected to greatly aid in the data quality of NEXRAD products used by the FAA weather systems. Those products are created from data processed to improve data quality of which hydrometeor classification could be a useful addition. This case though serves as a cautionary lesson regarding using a carte blanche approach. There may be risk of removal of convergence boundaries or other weather of note if all BI, AP, and GC class data are removed. Removing such data would certainly be harmful to the NEXRAD Machine Intelligent Gust Front Algorithm's (MIGFA) performance. Further study is warranted to determine how to appropriately apply HCA to the data quality problem.

Note in the HCA data (panel c) that at the far northeast extent of the squall line there is a sharp transition from lighter rain to wet snow classes. The data farther out show much variability. The range of this sharp transition is about 170 km from the radar. At this range, the sample volumes have become large. There is yet to be a useful range defined for any of the dual polarization parameters. Within the NEXRAD program, 200 km has been suggested as a likely maximum useful range.

### 3.2 SNOWFALL

Figure 2 depicts a snowfall case from December 22, 2004 at 1556 UTC. Reflectivity (panel a) has the characteristic look of a region of snow with clutter about the radar. The differential reflectivity (panel b) shows the expected low values with snow returns. Note the area southwest of the radar has higher values though. The HCA (panel c) classifies that region as crystals while the rest of the snow is a blend of crystals with dry snow. The specific differential phase shift (panel d) is non-descript. The correlation coefficient data (panel e) show highest values in regions coinciding with the higher reflectivity (panel a). Overall the  $\rho_{HV}$  values are lower than typically seen in rain situations.

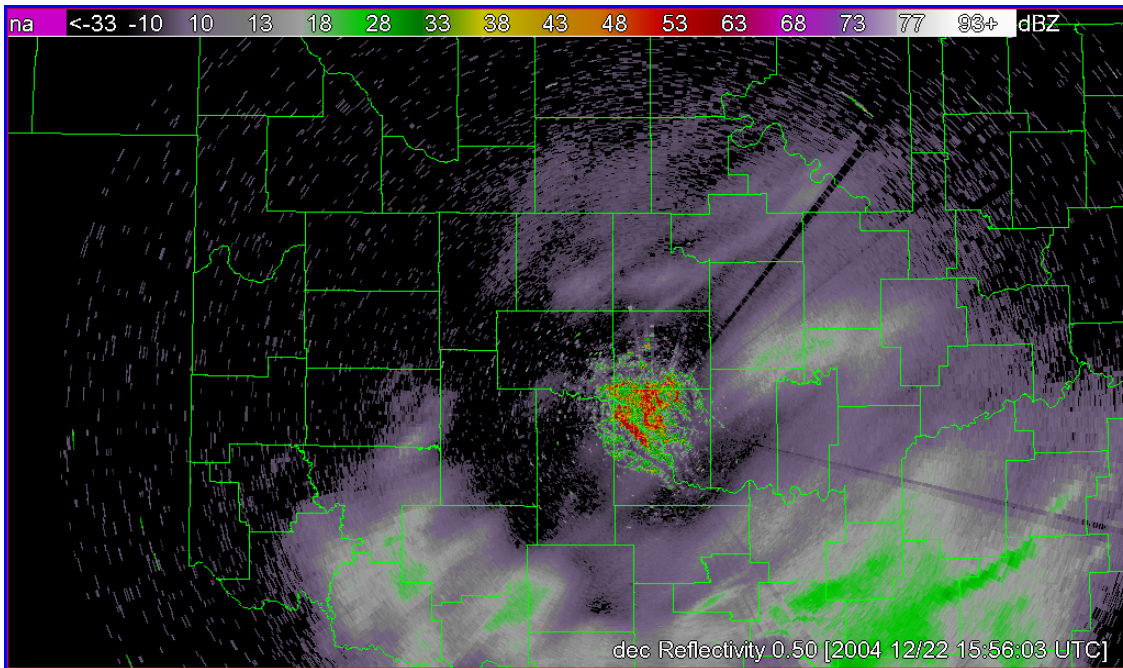


Figure 2a. Traditional reflectivity (dBZ) from the base tilt of the radar volume collected on December 22, 2004 at 1556 UTC. The scene depicts snowfall. Refer to section 3.2 for more detail.

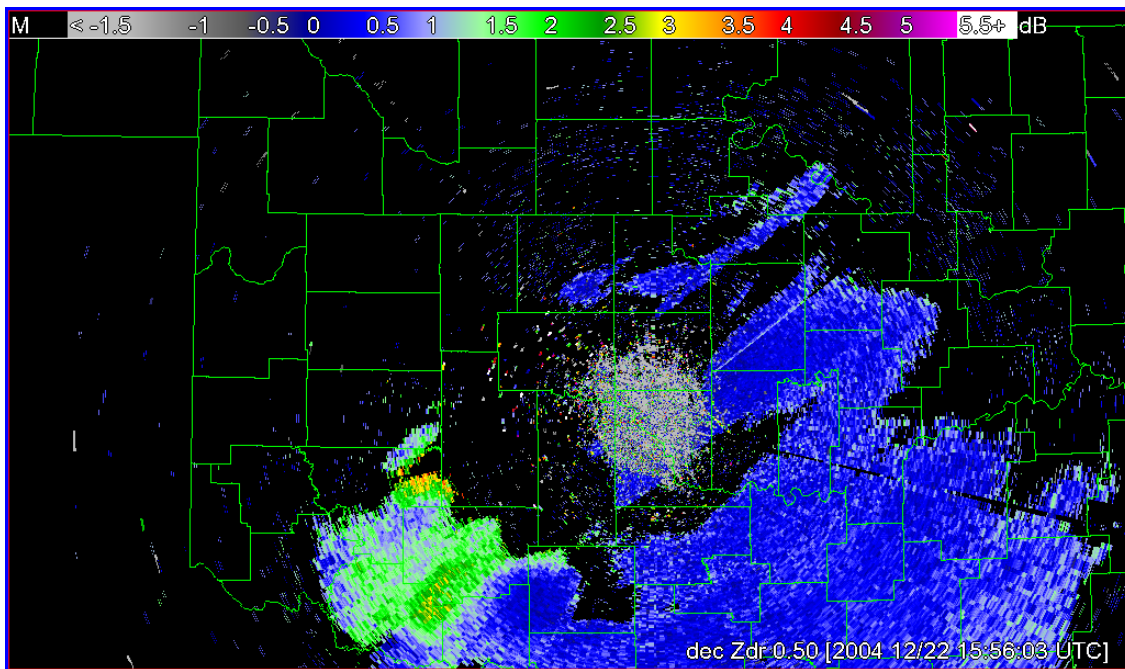


Figure 2b. Differential reflectivity (dB) from the base tilt of the radar volume collected on December 22, 2004 at 1556 UTC. The scene depicts snowfall. Snow yields low values of differential reflectivity. Refer to section 3.2 for more detail.

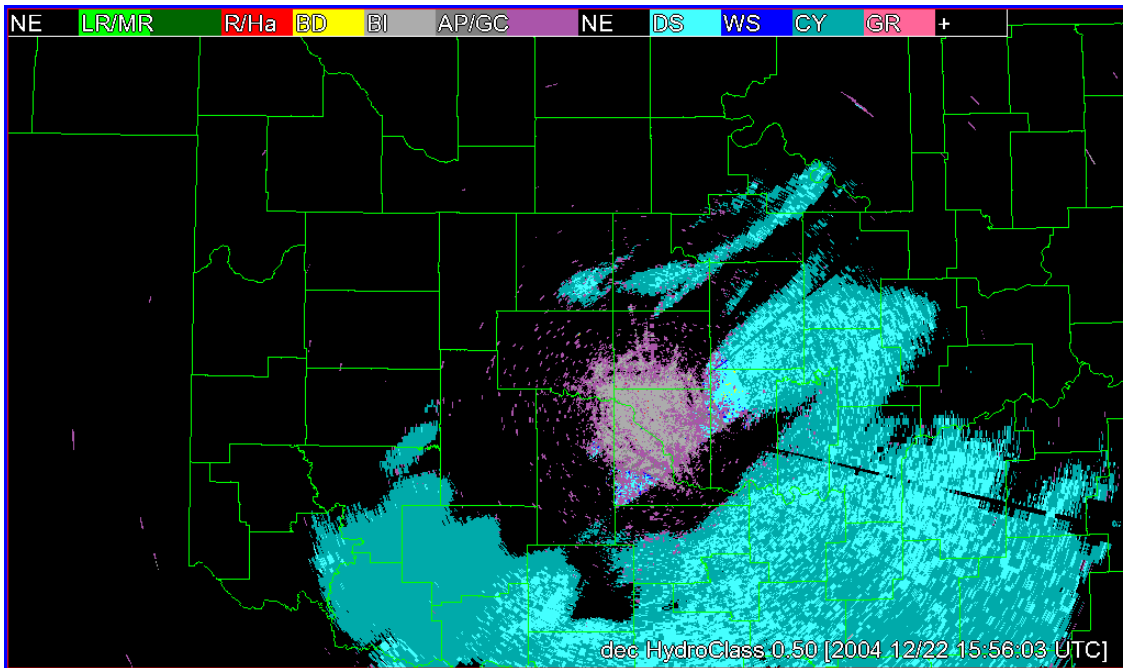


Figure 2c. Hydrometeor classification results for the base tilt of the radar volume collected on December 22, 2004 at 1556 UTC. The scene depicts snowfall. Decode the color scale as follows: black (NE – no echo), light green (LR – light rain), dark green (MR – medium intensity rain), red (R/Ha – heavy rain and/or hail), yellow (BD – big drops), gray (BI – biological targets), dark gray (AP – anomalous propagation), lavender (GC – ground clutter), light blue (DS – dry snow), dark blue (WS – wet snow), cyan (CY – ice crystals), and pink (GR – graupel). Refer to section 3.2 for more detail.

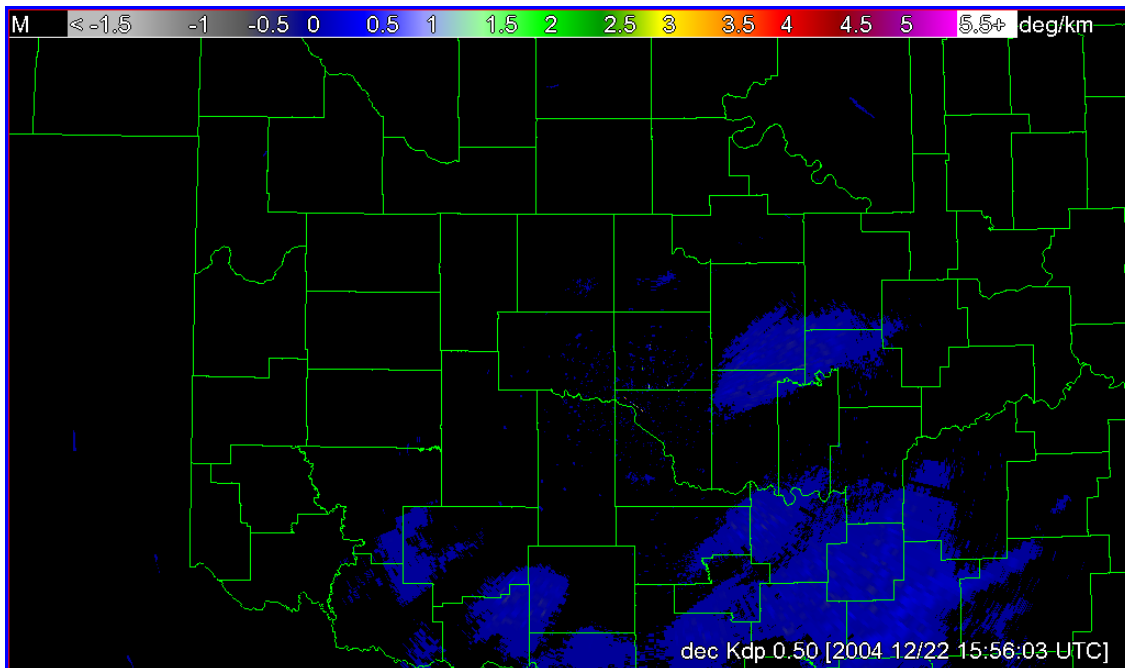


Figure 2d. Specific differential phase shift ( $K_{DP}$ ) in units of degrees/km for the base tilt of the radar volume collected on December 22, 2004 at 1556 UTC. The scene depicts snowfall. Refer to section 3.2 for more detail.

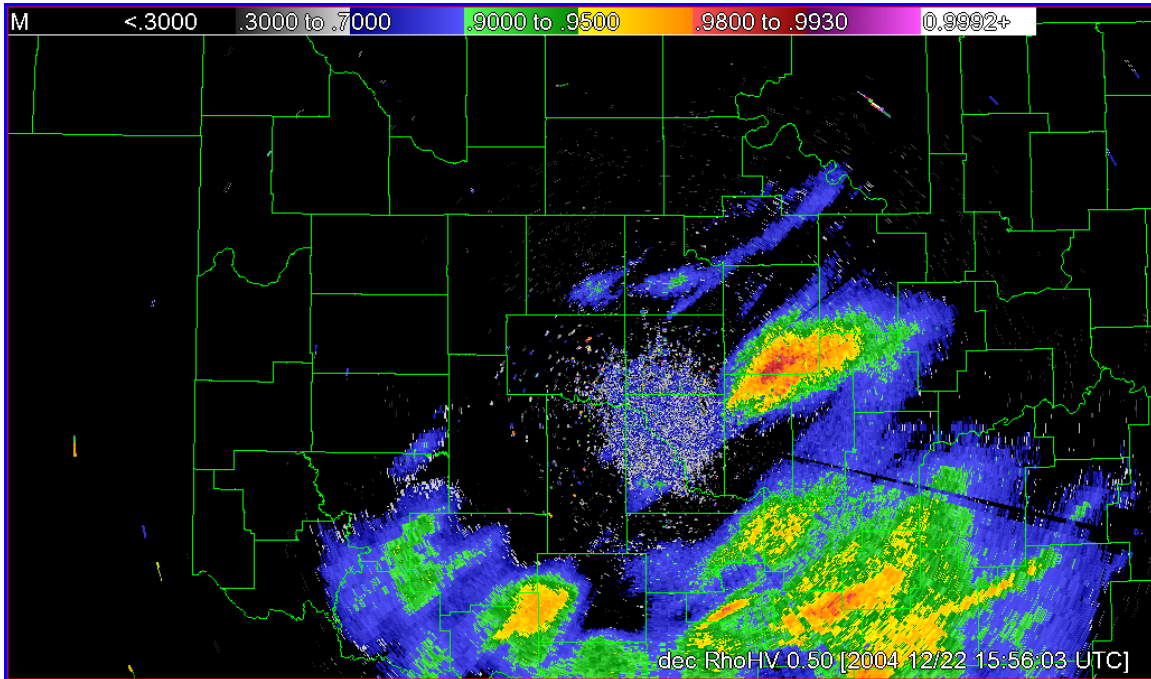


Figure 2e. Correlation coefficient ( $\rho_{HV}$ ) for the base tilt of the radar volume collected on December 22, 2004 at 1556 UTC. The scene depicts snowfall. This field has a small dynamic range near unity. For snow, the values are typically offset from unity a bit more than for rain. Refer to section 3.2 for more detail.

### 3.3 LIGHT RAIN AND BRIGHT BAND

A light rain case is presented in Figure 3 from May 2, 2005 at 1618 UTC. The panels depict data for the  $1.45^\circ$  elevation tilt (one cut above the base tilt) to highlight scanning through a melting layer bright band. The general ring of high reflectivity (panel a) centered about the radar is the bright band associated with a phase transition from solid to liquid water. This ring is at about 2000 feet elevation.  $Z_{DR}$  (panel b) is most pronounced in the general region of the bright band. At farther ranges, it is near zero indicative of light rain or snow. The bright band is readily observed as a ring of lowered correlation coefficient (panel e). These dual polarization parameters should bolster confidence for the identification of the bright band.

The HCA (panel c) shows a region of light rain generally below the bright band (closer ranges to the radar). In the same region as the reflectivity bright band, the HCA has big drops (BD, yellow) or rain/hail (R/Ha, red). Melting snowflakes would suddenly have much increased return as their phase transitions to liquid. To HCA, they seem to appear as the big drop class. The light rain class extends out beyond the bright band radius to a range of about 80 km. There the class assignment seems to artificially terminate. Beyond is a transition of a mix of snow types (wet and dry) and big drops. Obviously, the HCA somewhat struggles with the classes for this case. The consensus of reviewers in the evaluation study was that HCA is problematic in the big drop/wet snow classes.

In another case (not shown), ground observations did not mesh well when dealing with these particular classes. There were surface-to-aloft class mismatches. It is certainly possible to have wet snow at lower radar volume tilts be realized as rain at the surface. It is virtually impossible though for big drops at low tilts to transition to snow at the surface.

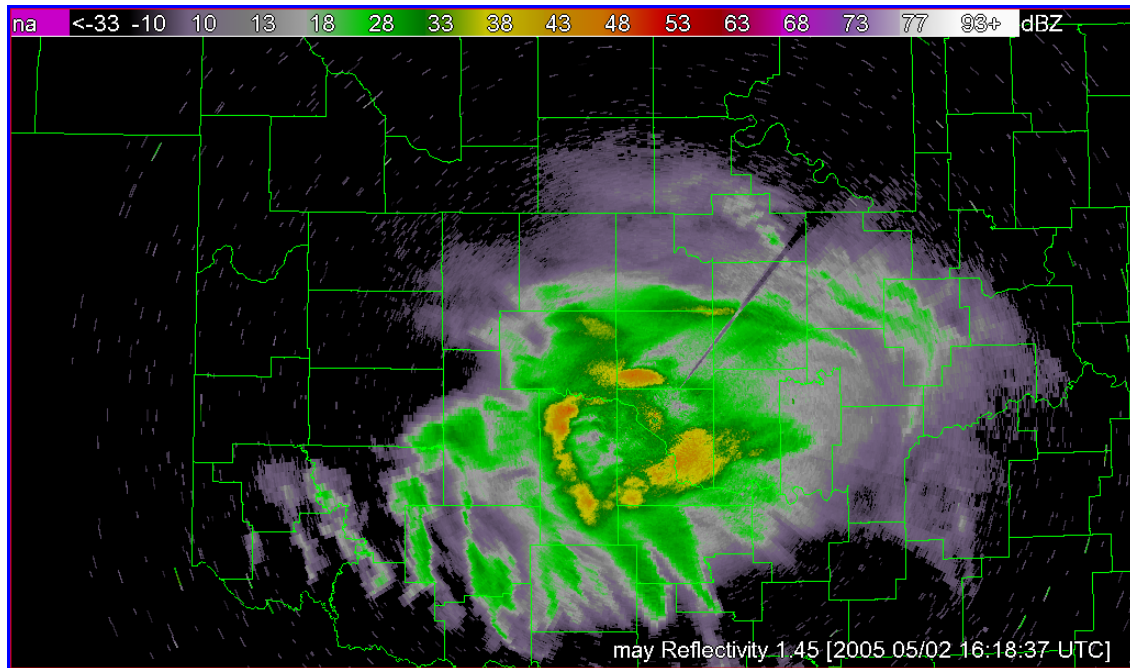


Figure 3a. Traditional reflectivity (dBZ) from the  $1.45^\circ$  tilt of the radar volume collected on May 2, 2005 at 1618 UTC. The scene depicts light rain with a melting layer bright band. Refer to section 3.3 for more detail.

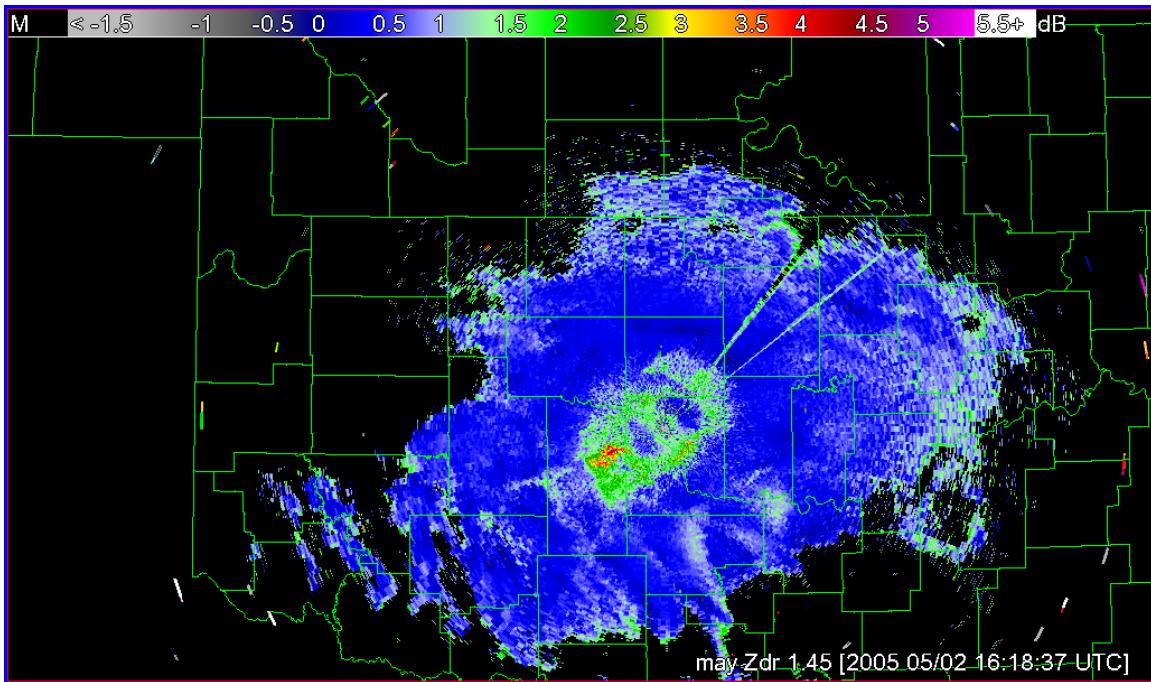


Figure 3b. Differential reflectivity (dB) from the 1.45° tilt of the radar volume collected on May 2, 2005 at 1618 UTC. The scene depicts light rain with a melting layer bright band. The higher values of differential reflectivity are associated with the bright band. Refer to section 3.3 for more detail.

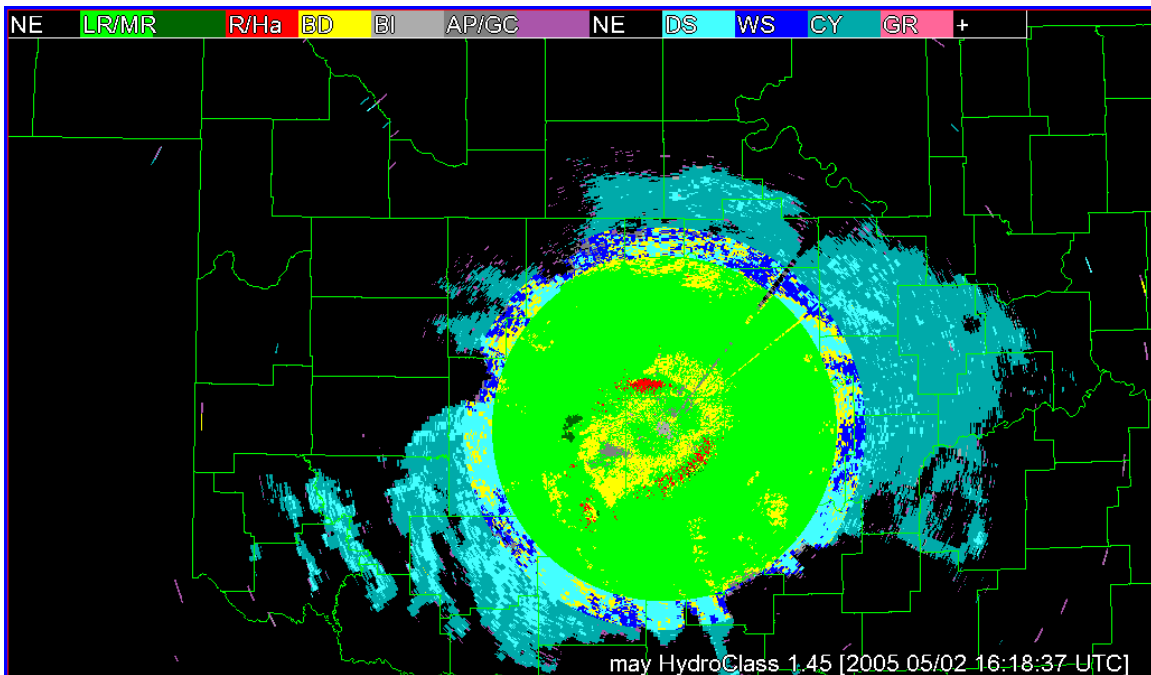


Figure 3c. Hydrometeor classification results for the 1.45° tilt of the radar volume collected on May 2, 2005 at 1618 UTC. The scene depicts light rain with a melting layer bright band. Decode the color scale as follows: black (NE – no echo), light green (LR – light rain), dark green (MR – medium intensity rain), red (R/Ha – heavy rain and/or hail), yellow (BD – big drops), gray (BI – biological targets), dark gray (AP – anomalous propagation), lavender (GC – ground clutter), light blue (DS – dry snow), dark blue (WS – wet snow), cyan (CY – ice crystals), and pink (GR – graupel). Refer to section 3.3 for more detail.

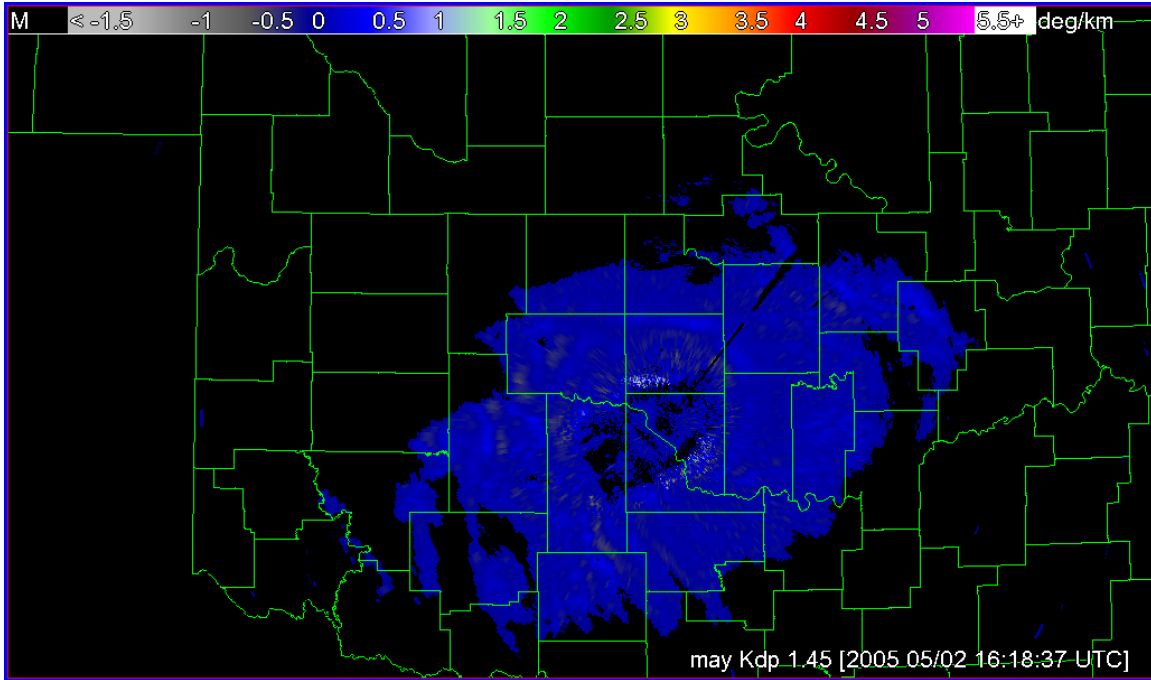


Figure 3d. Specific differential phase shift ( $K_{DP}$ ) in units of degrees/km for the  $1.45^\circ$  tilt of the radar volume collected on May 2, 2005 at 1618 UTC. The scene depicts light rain with a melting layer bright band. Refer to section 3.3 for more detail.

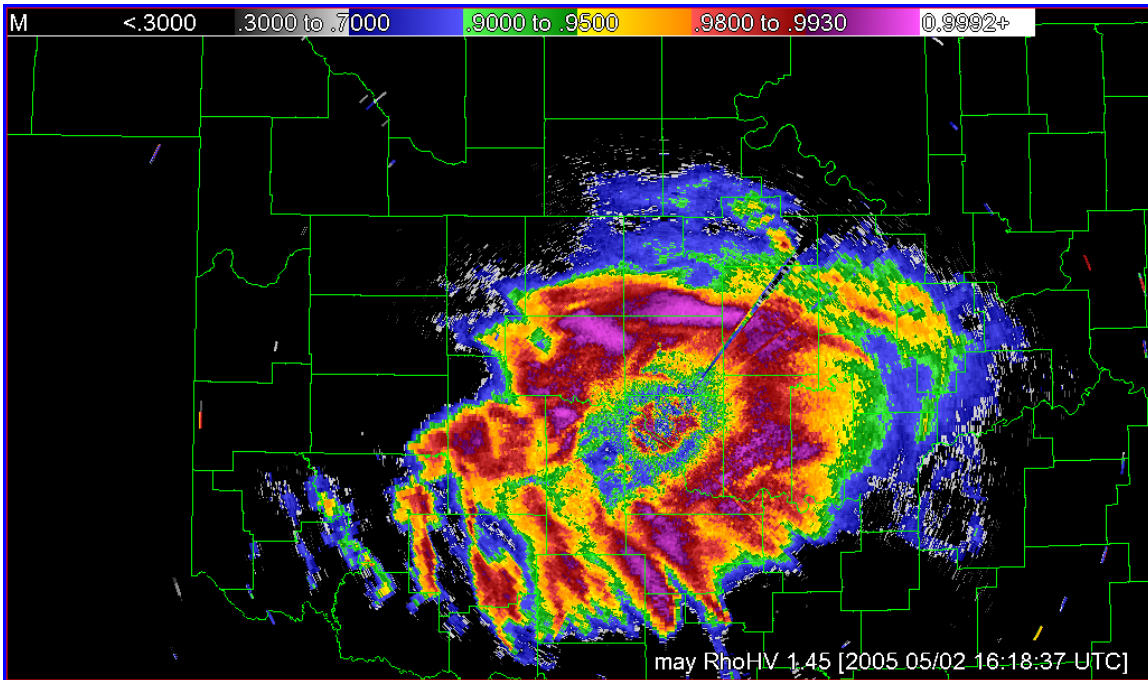


Figure 3e. Correlation coefficient ( $\rho_{HV}$ ) for the  $1.45^\circ$  tilt of the radar volume collected on May 2, 2005 at 1618 UTC. The scene depicts light rain with a melting layer bright band. This field has a small dynamic range near unity. The bright band is notable as lower values within a broad region of higher values. Refer to section 3.3 for more detail.

### 3.4 FREEZING RAIN

Figure 4 is a case of freezing rain northwest of the radar from January 5, 2005 at 0541 UTC. The stronger reflectivity (panel a) is associated with higher values of differential reflectivity (panel b), a classification (panel c) of graupel (GP, pink), and lower correlation coefficient (panel e). This broad region is within a lower reflectivity precipitation swath of nearer zero differential reflectivity associated with the snow and ice crystal classes. At the surface, rain transitioned to freezing rain with pockets of stronger precipitation also containing ice pellets. The dual polarization analysis of this situation cannot explain the surface observations of rain and freezing rain. There is no way to know of melting or refreezing beneath the lowest tilt of the radar volume. Assuming the HCA snow and ice crystal classes are correct, a phase transformation to liquid from solid would physically require a layer of above freezing temperatures between the low tilt scan of the radar and the surface. A very shallow, below freezing layer at the surface also has to develop for freezing rain conditions. Obviously, the radar cannot determine the evolution of this temperature structure. This, and the prior case, indicates HCA should not be used solely for determining surface weather conditions in the terminal airspace. This suggests a multi-sensor approach may be necessary for useful application of HCA information. Surface reports, pilot reports, and atmospheric profiles from meteorological models should be used to enhance the value of the HCA.

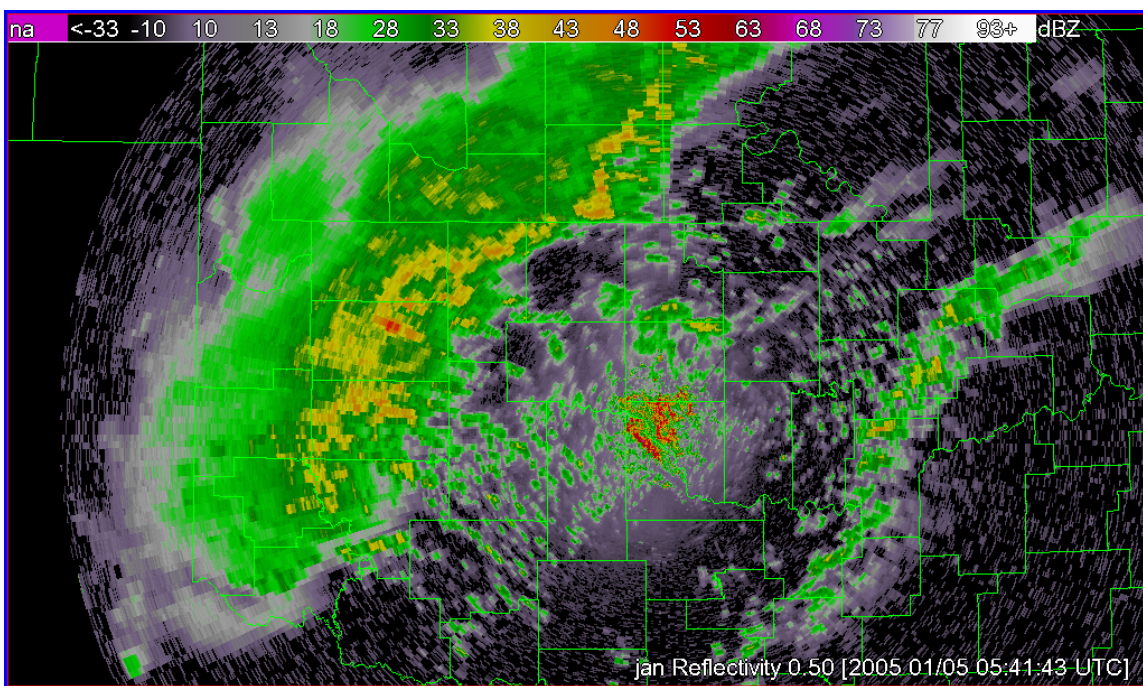


Figure 4a. Traditional reflectivity (dBZ) from the base tilt of the radar volume collected on January 5, 2005 at 0541 UTC. The scene depicts freezing rain northwest of the radar (center). Refer to section 3.4 for more detail.



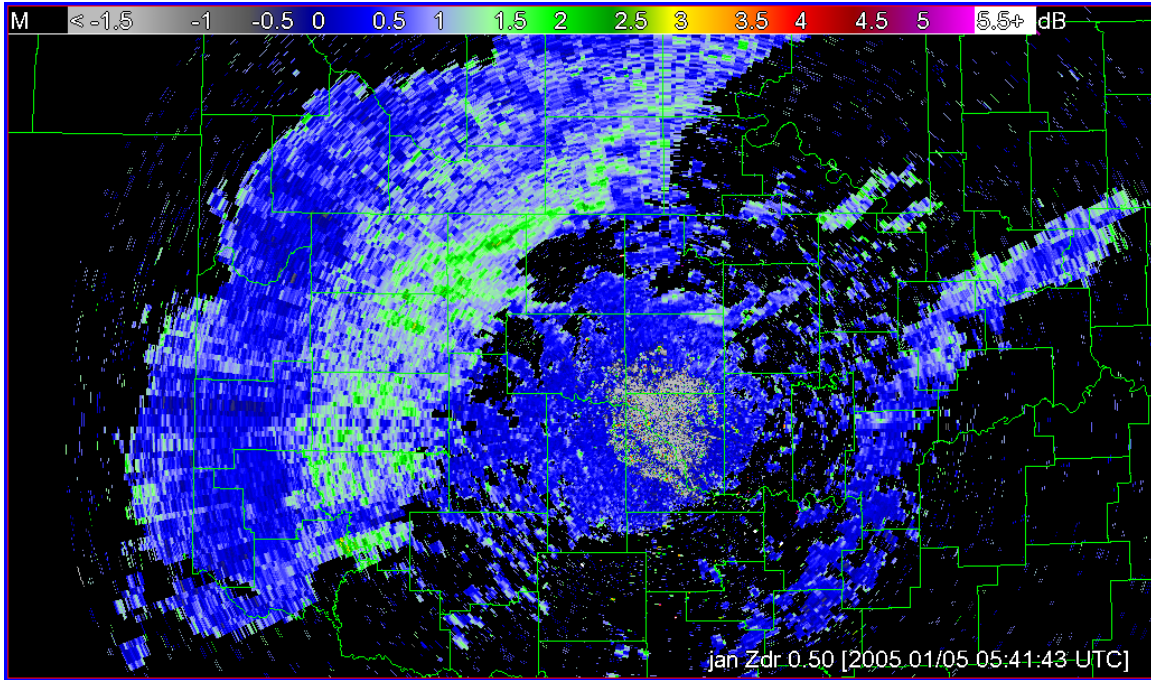


Figure 4b. Differential reflectivity (dB) from the base tilt of the radar volume collected on January 5, 2005 at 0541 UTC. The scene depicts freezing rain northwest of the radar (center). Refer to section 3.4 for more detail.

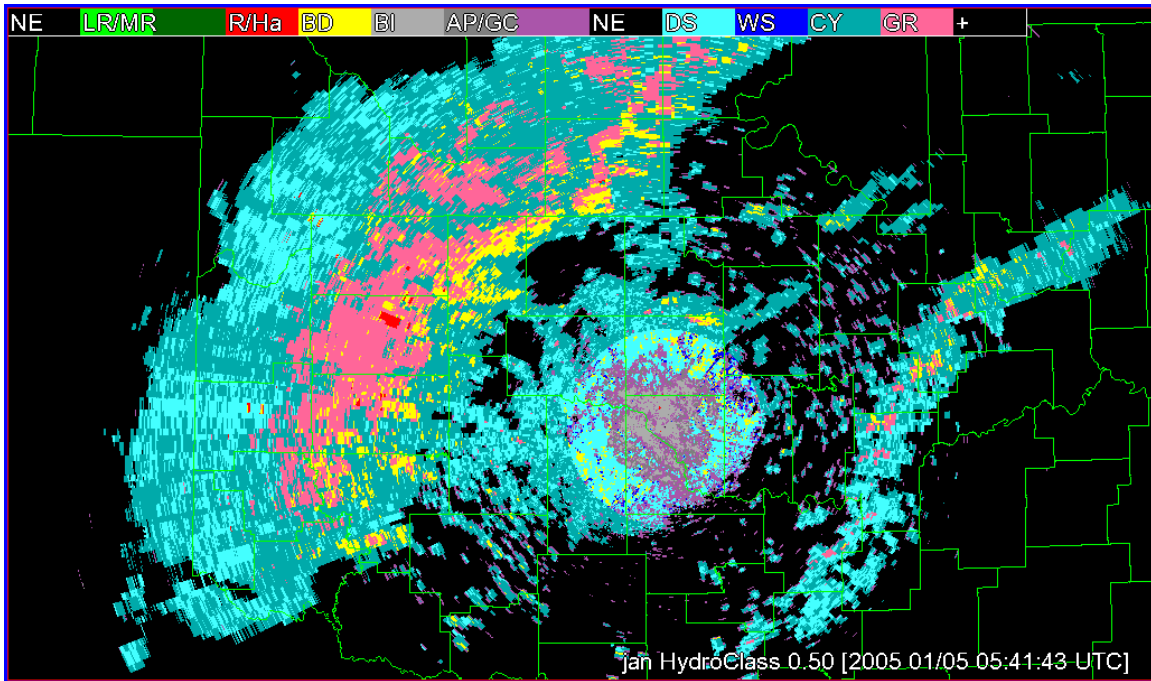


Figure 4c. Hydrometeor classification results for the base tilt of the radar volume collected on January 5, 2005 at 0541 UTC. The scene depicts freezing rain northwest of the radar (center). Higher intensity precipitation in Figure 4a coincides with the graupel (pink) classification. Decode the color scale as follows: black (NE – no echo), light green (LR – light rain), dark green (MR – medium intensity rain), red (R/Ha – heavy rain and/or hail), yellow (BD – big drops), gray (BI – biological targets), dark gray (AP – anomalous propagation), lavender (GC – ground clutter), light blue (DS – dry snow), dark blue (WS – wet snow), cyan (CY – ice crystals), and pink (GR – graupel). Refer to section 3.4 for more detail.

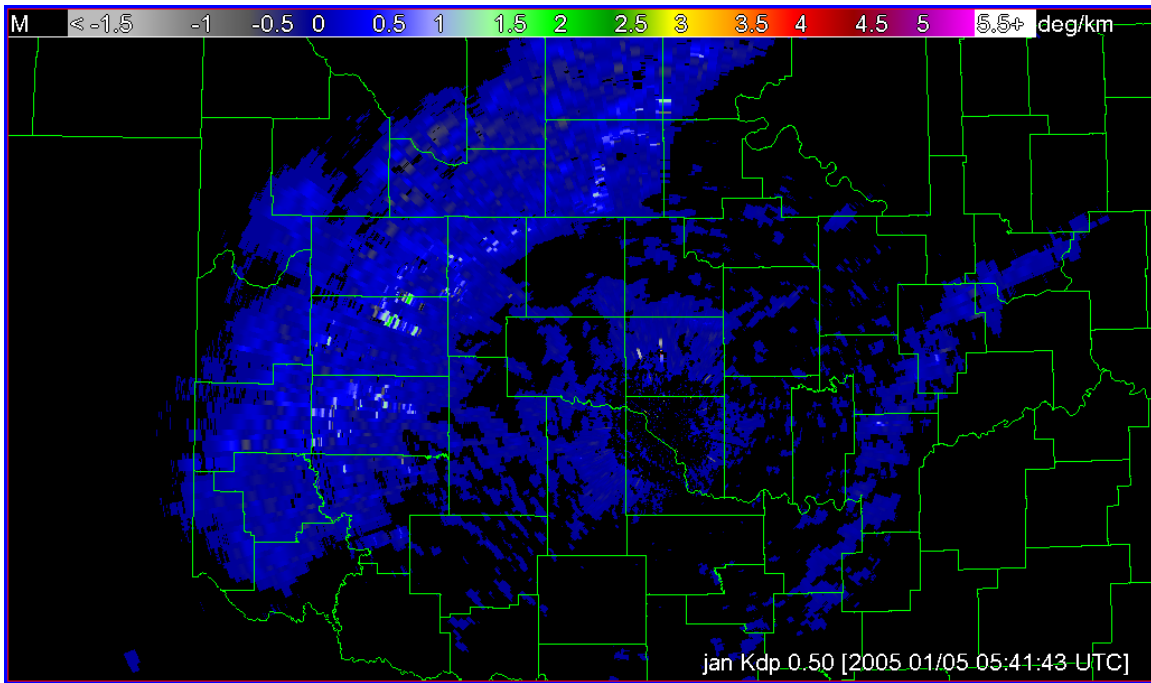


Figure 4d. Specific differential phase shift ( $K_{DP}$ ) in units of degrees/km for the base tilt of the radar volume collected on January 5, 2005 at 0541 UTC. The scene depicts freezing rain northwest of the radar (center). Refer to section 3.4 for more detail.

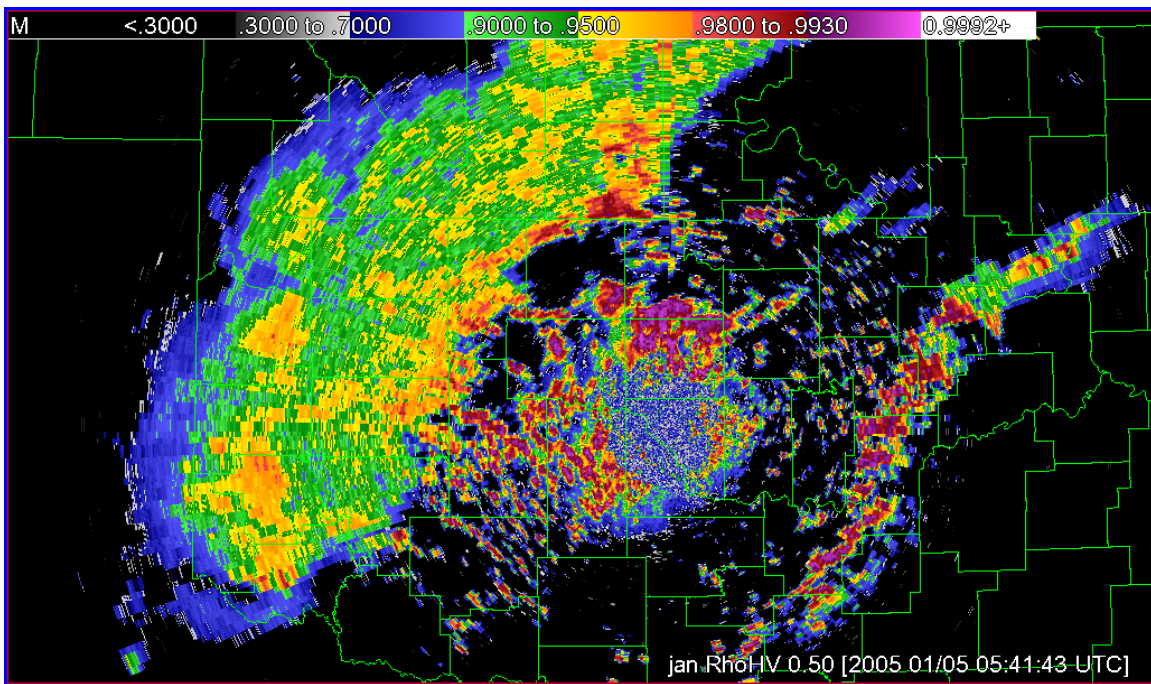


Figure 4e. Correlation coefficient ( $\rho_{HV}$ ) for the base tilt of the radar volume collected on January 5, 2005 at 0541 UTC. The scene depicts freezing rain northwest of the radar (center). This field has a small dynamic range near unity. Refer to section 3.4 for more detail.



## 4. SUMMARY

The dual polarization upgrade of NEXRAD will yield three new base parameters and two derived parameters. From this, a new capability to better understand the bulk scatterers of a sample volume and their evolution will be possible. The first use of this new capability is to improve on quantitative precipitation estimates. The NEXRAD program is doing this through incorporation of an algorithm developed at NSSL. This incorporation process includes components that will make dual polarization data available to other algorithms. On behalf of the NEXRAD program, NSSL coordinated the evaluation of dual polarization data from seven weather cases. The purpose of the evaluation is to begin the process of defining other new NEXRAD dual polarization products and the nature of the dual polarization data that will be made available to other algorithms.

The potential benefit of the NEXRAD dual polarization upgrade to FAA weather systems begins with participation in the evaluation of the seven cases. Examples from four cases are illustrated in this report. These cases were chosen to focus on aviation weather hazards: convection and outflow boundaries, winter weather, melting layer bright bands, and freezing rain. The analysis suggests a multi-sensor approach may heighten the utility of using some of the newer dual polarization information. The benefit to FAA weather systems is not likely to be direct but from a new class of automated dual polarization algorithms to augment existing products or create new ones. A number of observations summarize this report.

1. Many more dual polarization cases are needed from many more regions of the U.S. This will further the understanding of the potential benefit from the five new dual polarization parameters. It will yield increased confidence in those that perform well. The HCA algorithm likely will benefit from a more diverse data ensemble; particularly to further development of class distinctions between wet snow and big drops. Robust, automated algorithms developed for the new dual polarization parameters require diverse data cases for testing.
2. The ability of HCA to identify biological targets, AP, and ground clutter in the radar returns can be beneficial to improving NEXRAD data quality. By removing such contaminants, products used in CIWS and ITWS such as High Resolution VIL (HRVIL) and High Resolution Enhanced Echo Tops (HREET) should be improved. However, the use of HCA to improve data quality may not be straight-forward. In this very limited set of evaluation cases, a long-lived outflow boundary was classified as AP.
3. Current weather system products may be improved or augmented. Besides potential data quality benefits from HCA, the ability to detect the bright band and classes of meteorological scatterers may have uses with existing products. HRVIL may be “decontaminated” by removal of bright band and hail contributions. Classification of winter weather types could benefit from HCA. However, relating conditions in a radar volume to weather type at the surface will require additional information beyond HCA. Focusing on specific differential phase shift ( $K_{DP}$ ) peaks and trends in conjunction with HRVIL and HREET could contribute to predicting convective growth and decay.

4. New weather system products may be possible. One benefit of the dual polarization upgrade is improving on QPE. That is done by incorporating multiple “Z-R” relationships keyed to the classes of precipitation identified by HCA. Similarly, different “VILs” could be developed based on classification. These could be used to determine intensities associated from the class contributors. Trending of such information may have value regarding feature growth and decay. This could also be used with supporting environmental data to identify regions with icing potential (drops at altitudes above the freezing layer).

## GLOSSARY

AP	Anomalous Propagation
CIWS	Corridor Integrated Weather System
FAA	Federal Aviation Administration
HCA	Hydrometeor Classification
HREET	High Resolution Enhanced Echo Tops
HRVIL	High Resolution VIL
ITWS	Integrated Terminal Weather System
NEXRAD	Next Generation Weather Radar
NSSL	National Severe Storms Laboratory
ORPG	Open Radar Product Generator
QPE	Quantitative Precipitation Estimate



## REFERENCES

- Bringi, V. N., and V. Chandrasekar, 2001: Polarimetric Doppler Weather Radar: Principles and Applications. Cambridge University Press, Cambridge, UK, 662 pp.
- Lakshmanan, V., T. Smith, G. J. Stumpf, and K. Hondl, 2007: The Warning Decision Support System - Integrated Information (WDSS-II). *Weather and Forecasting*, to be published.
- Ryzhkov, A., T. J. Schuur, D. W. Burgess, P. L. Heinselman, S. E. Giangrande, and D. S. Znić, 2005: The Joint Polarization Experiment: Polarimetric rainfall measurements and hydrometeor classification. *Bull. Amer. Meteor. Soc.*, **86**, 809–824.
- Salek, M., J-L. Cheze, J. Handwerker, L. Delobbe, and R. Uijlenhoet, 2004: Radar Techniques for Identifying Precipitation Type and Estimating Quantity of Precipitation. Document of COST Action 717, WG 1, 51 pp.
- Scharfenberg, K., and K. L. Manross, 2007: A Product Evaluation for the Dual-Polarimetric WSR-88D. Report of the National Severe Storms Laboratory, 31 pp.